

Avoided criticality and slow relaxation in frustrated two-dimensional models

Ilya Esterlis^{*} and Steven A. Kivelson[†]*Department of Physics, Stanford University, Stanford, California 94305, USA*Gilles Tarjus[‡]*LPTMC, CNRS-UMR 7600, Université Pierre et Marie Curie, 4 Place Jussieu, 75252 Paris Cedex 05, France*

(Received 12 June 2017; revised manuscript received 1 September 2017; published 23 October 2017)

Frustration and the associated phenomenon of “avoided criticality” have been proposed as an explanation for the dramatic relaxation slowdown in glass-forming liquids. To test this, we have undertaken a Monte Carlo study of possibly the simplest such problem, the two-dimensional XY model with frustration corresponding to a small flux f per plaquette. At $f = 0$, there is a Berezinskii-Kosterlitz-Thouless transition at T^* , but at any small but nonzero f , this transition is avoided and replaced (presumably) by a vortex-ordering transition at much lower temperatures. We thus have studied the evolution of the dynamics for small and moderate f as the system is cooled from above T^* to below. Although we do find strongly temperature-dependent slowing of the dynamics as T crosses T^* and that simultaneously the dynamics becomes more complex, neither effect is anywhere nearly as dramatic as the corresponding phenomena in glass-forming liquids. At the very least, this implies that the properties of supercooled liquids must depend on more than frustration and the existence of an avoided transition.

DOI: [10.1103/PhysRevB.96.144305](https://doi.org/10.1103/PhysRevB.96.144305)

I. INTRODUCTION

The quest for a simple compelling theoretical framework for understanding the spectacular dynamical phenomena exhibited “universally” by supercooled liquids as they approach the glass transition has been long and arduous [1–3]. Surely the most dramatic of these phenomena is the super-Arrhenius temperature (T) dependence of the relaxation rates in the range of T between the melting temperature and the glass transition temperature T_g . One set of theoretical ideas seeks to identify these dynamical phenomena with the growth of thermodynamic correlations of some sort with the notion that geometric frustration f can be invoked to account for ultimately limiting the growth of these correlations and precluding a transition to a broken symmetry (crystalline) state [4–6]. Specifically, one concrete proposal of this variety suggests that the phenomena should be thought of as deriving from proximity to an “avoided critical point” T^* , a point at which a transition to an “ideal” solid phase would occur in the absence of frustration but which is forbidden for any nonzero f [7–10].

At the most optimistic level, one could then hope that any model with tunable frustration and an avoided critical point would automatically show the salient features of supercooled liquids. Besides the already mentioned spectacular increase of the relaxation time, whose temperature dependence is described by a super-Arrhenius form, the main qualitative features that one would like to reproduce are a nonexponential time dependence of the relaxation functions and the appearance of several relaxation regimes, both effects becoming more marked as one cools the liquid toward the glass transition. To test this, we have undertaken a Monte Carlo study of possibly the simplest such problem, the two-dimensional (2D) XY model with frustration corresponding to a small flux f per

plaquette. At $f = 0$, there is a Berezinskii-Kosterlitz-Thouless (BKT) transition at $T^* \approx 0.89J$, but at any small but nonzero f , this transition is avoided and replaced (presumably) by a vortex-ordering transition at much lower temperatures. We thus have studied the evolution of the (Monte Carlo) dynamics for small f as the system is cooled from above T^* to below.

Although we do find strongly temperature-dependent slowing of the dynamics as T crosses T^* and that simultaneously the dynamics becomes more complex (i.e., not describable as a single exponential), neither effect is anywhere nearly as dramatic as the corresponding phenomena in supercooled liquids. At the very least, this implies that the properties of supercooled liquids must depend on more than the mere existence of an avoided transition. Conversely, it should be mentioned that, in the slightly more involved example of a one-component atomic liquid in curved space (where the curvature of space is a measure of the frustration f), the properties near T^* much more closely resemble those of supercooled liquids, including the occurrence of a range of temperatures in which super-Arrhenius slowing down is observed [11,12].

II. MODEL AND SIMULATIONS

The Hamiltonian of the uniformly frustrated 2D XY model is given by [13]

$$H = -J \sum_{\langle ij \rangle} \cos(\theta_i - \theta_j - A_{ij}), \quad (1)$$

where $J > 0$ is the coupling constant, θ_i is the angle of the XY spin at site i , and $\langle ij \rangle$ denotes a sum over distinct pairs of nearest-neighbor sites. The bond variables A_{ij} satisfy the constraint that their sum going counterclockwise around any unit-cell C of the lattice is constant,

$$\sum_C A_{ij} = 2\pi f, \quad (2)$$

where without loss of generality, f can be restricted to the range of $[0, 1/2]$. Here we consider a square lattice.

^{*}ilyae@stanford.edu
[†]kivelson@stanford.edu[‡]tarjus@lptmc.jussieu.fr

The same model has been used to describe an array of Josephson junctions in a uniform transverse magnetic field [13,14]; in this case the A_{ij} 's can be interpreted, up to some constant prefactor, as the line integral of the vector potential along the bonds, and f is the number of flux quanta of magnetic field per unit cell [14].

The system is *frustrated* in that nonzero f , no matter how small, induces an irreducible density of topological defects, i.e., vortices all of the same sign. Whereas the 2D XY model (i.e., the model with $f = 0$) undergoes the well-known BKT transition to a low-temperature state with quasi-long-range order at $T = T^*$, for nonzero f the gas of irreducible defects eliminates this transition. These defects can crystallize, resulting in an ordered state analogous to the Abrikosov vortex lattice in a type-II superconducting film, but this transition occurs at a temperature T_{crys} that is more than an order of magnitude lower than T^* in the limit of small frustration f [15–17]. The parameter f therefore quantifies the frustration that is present in the system. This frustration is not associated with site-dependent quenched disorder: It is *uniform*. Furthermore, because the Hamiltonian in Eq. (1) is gauge invariant, physical properties depend on the A_{ij} 's only through f [18].

We have investigated the uniformly frustrated 2D XY model described by Eq. (1) for small-to-intermediate frustration f both by analytical and by numerical approaches. We have performed Monte Carlo simulations for linear size $L = 34$ with several values of the frustration, $f = n/L^2$ where n is the irreducible number of flux quanta, corresponding to $f = 5/34^2, 10/34^2, 1/34, 5/34, \text{ and } 13/34$. (Recall that the maximum value is $f = 1/2$ which corresponds to the so-called “fully frustrated” XY model [14].)

Our Monte Carlo simulation uses single-site updates in which each spin variable is updated according to the Metropolis method. (This corresponds to a “model-A” [19] dynamics for a nonconserved order parameter.) Spins are updated by selecting a random angle with a range chosen to maintain an acceptance ratio of approximately 0.5. A single sweep corresponds to updating each spin once. In the simulations discussed here, correlation functions were measured after every sweep. We have used a gauge choice such that $A_{ij} = 0$ for vertical bonds and $A_{ij} = 2\pi f y_i$ for horizontal bonds, where y_i is the ordinate of site i . We also have studied the system in the absence of frustration ($f = 0$) as a function of system size for $L = 10\text{--}40$.

In the present paper, we have concentrated on dynamical rather than spatial correlations. We have therefore computed the spatially averaged spin-spin autocorrelation function,

$$\begin{aligned} C_{ss}(t) &\equiv \frac{1}{L^2} \sum_{i=1}^{L^2} \langle \mathbf{S}_i(0) \cdot \mathbf{S}_i(t) \rangle \\ &= \frac{1}{L^2} \sum_{i=1}^{L^2} \langle \cos[\theta_i(0) - \theta_i(t)] \rangle, \end{aligned} \quad (3)$$

and the current-current autocorrelation function,

$$C_{jj} \equiv \frac{1}{L^2} \sum_{i=1}^{L^2} \langle \sin \Theta_i(0) \sin \Theta_i(t) \rangle, \quad (4)$$

where

$$\Theta_i(t) \equiv \theta_i(t) - \theta_{i+\hat{x}}(t) - A_{i,i+\hat{x}}. \quad (5)$$

Autocorrelation functions were computed by averaging over 100–1000 configurations, depending on temperature and frustration.

III. AVOIDED CRITICALITY: PREDICTIONS FOR THE DYNAMICS

We consider the dynamical behavior of the system when it relaxes to equilibrium in the limit of small frustration $f \rightarrow 0^+$. As mentioned above, there is a large range of temperature from around T^* down to T_{crys} . In the unfrustrated model ($f = 0$), the physics near and below T^* can be described in terms of thermally induced defects (vortices) of both positive and negative topological charges subject to a global constraint of charge neutrality. The density of these defects decreases with decreasing temperature, and below T^* they only appear in dipoles formed by pairs of two nearby oppositely charged defects. The system then displays quasi-long-range order. The defect picture can be introduced conveniently through the duality transformation that modulo some approximations maps the original model of XY spins into a Coulomb lattice gas now with the vortices as variables.

For $f \neq 0$, but small, the system may locally have a tendency to behave as if unfrustrated, but this cannot extend beyond an intrinsic frustration length which is of the order of $\ell = f^{-1/2}$. Indeed, frustration-induced defects must be present in addition to thermally generated ones, and the irreducible density of such vortices, which all have the same topological charge of $+1$, is precisely f . One may therefore expect that, for some range of temperatures near and below T^* and in the limit of small f , the frustrated model behaves as an unfrustrated one in a box of linear size of the order of $\ell = f^{-1/2}$ (with periodic boundary conditions). This is indeed what has been found for the thermodynamic properties [20].

At still lower temperatures but above the freezing transition to a vortex lattice, the system should behave as a fluid of $+1$ vortices with density f in a neutralizing background, i.e., a “one-component plasma.” The vortices interact with the 2D lattice Coulomb potential V , which at large separation r has a logarithmic dependence: $V(r) \sim -2\pi J \ln(r/a)$ with a of the order of a lattice constant.

To make progress we first derive the finite-size scaling of the dynamics of the unfrustrated model ($f = 0$) in the region below T^* which is dominated by spin-wave excitations. The magnetization in a finite-size system of linear size L has a characteristic magnitude of $M_\infty \simeq L^{-\eta(T)/2}$ with $\eta(T) = T/(2\pi J)$ [21,22]. One may then define two different time scales: A first time τ_1 to go from a magnetization of order $O(1)$ to a magnetization of order M_∞ and a second one τ_2 , which characterizes the long-time orientational fluctuations of the magnetization.

The first time τ_1 is given by standard finite-size scaling to be $\tau_1 \sim L^z$ with z as the dynamical exponent corresponding here to model A, i.e., $z = 2$. This is also obtained as the time for the spin-spin autocorrelation function to decay from 1 to $(M_\infty)^2$. In this regime, the time-dependent correlation function decays

as $t^{-\eta(T)/2}$ for the present dynamics, which leads indeed to

$$\tau_1(L) \sim [L^{-\eta}]^{-(2/\eta)} \sim L^2, \quad (6)$$

with τ_1 roughly independent of the temperature.

The second time τ_2 is associated with the relaxation of the magnetization angle $\theta(t)$. Since the process is akin to a random walk, the number of Monte Carlo steps per spin that are necessary to rotate the angle by an amount of order 2π goes as $(2\pi)^2 / \langle (\delta\theta)^2 \rangle$ where $\langle (\delta\theta)^2 \rangle = \int d\delta \delta\theta (\delta\theta)^2 p(\delta\theta)$ with $p(\delta\theta)$ as the probability that an angular change $\delta\theta$ is made.

The probability $p(\delta\theta)$ is given by a Boltzmann factor involving the free-energy change associated with the angular change. Large angular changes are thus strongly (exponentially) suppressed at low temperatures. We therefore consider a twist of small amplitude $2\pi\delta$ in one direction across the sample such that $\theta(x, y) = (2\pi\delta/L)x$. The associated free-energy change is given by $(J/2) \iint dx dy [\partial\theta(x, y)]^2 \sim (2\pi^2 J)\delta^2 \sim \kappa\delta^2$ with κ as a constant. One then estimates the mean-squared angle change as

$$\langle (\delta\theta)^2 \rangle \sim (2\pi)^2 \int_0^{\delta_c} d\delta \delta^2 e^{-(\kappa\delta^2/T)}, \quad (7)$$

where δ_c is a cutoff value. At low temperatures, the above expression behaves as $T^{3/2}$, and the relaxation time τ_2 then scales as

$$\tau_2(L, T) \sim L^2 \left(\frac{T^*}{T} \right)^{3/2}, \quad (8)$$

where L^2 accounts for the number of spins in the system. Note that as expected $\tau_2(L, T) > \tau_1(L)$ below T^* .

After putting together the above results, one obtains that the spin-spin autocorrelation function behaves in the following way:

$$C_{ss}(t) \sim \begin{cases} t^{-(\eta/2)} & \text{for } t \ll \tau_1, \\ \tau_1^{-(\eta/2)} e^{-(t-\tau_1)/\tau_2} & \text{for } t \gg \tau_1. \end{cases} \quad (9)$$

Note that the exponent $\eta(T) = T/(2\pi J)$ decreases as T decreases so that the initial slope of $C_{ss}(t)$ versus $\log(t)$ becomes less and less negative as T decreases. In the macroscopic limit $L \rightarrow \infty$, $\tau_1(L) \rightarrow \infty$, and $C_{ss}(t) \sim t^{-\eta(T)/2}$ at all times as required.

What are the consequences for the frustrated model? As explained above, for a range of temperatures near and below T^* , we expect that the behavior of the weakly frustrated ($f \ll 1$) model in the thermodynamic limit is similar to that of the unfrustrated model in a finite-size box of linear size of the order of the intrinsic frustration length, i.e., $L \approx \ell = f^{-1/2}$. The above predictions should thus apply provided one replaces L by ℓ . For the thermodynamic quantities, Alba *et al.* [20] have found that the finite-size scaling with $L \approx f^{-1/2}$ describes their numerical simulations from $T^* \approx 0.89J$ down to $T = 0.2J$, which is the lowest temperature they considered. However, they did not address the validity of this scaling analysis for the dynamics.

At still lower temperatures (but above T_{crys}), we expect to see behavior characteristic of a one-component plasma of density f . In the low-temperature correlated-fluid regime of the three-dimensional (3D) one-component plasma, it has been observed that the dynamics can be described as an

activated process with a relaxation time following an Arrhenius temperature dependence [23]. One might anticipate a similar behavior in two dimensions.

When vortices form a dilute gas, i.e., when the frustration $f \rightarrow 0^+$, their motion is nonetheless thermally activated at low temperatures because of the periodic pinning potential associated with the (essentially) ordered spins on the underlying lattice [16,17,24]. This is analogous to the Peierls potential for dislocations in a crystal. This activation energy has been estimated by Lobb *et al.* [24] and found to be of the order of $0.19J$ for a square lattice: This activation barrier can therefore be felt only if the system can be cooled in a disordered phase to very low temperatures significantly below $0.19J$. (Note that T_{crys} has been estimated to be around $0.045J$ [16,17].)

For a larger but still small density f , the one-component plasma is in a fluid phase, and the activation barrier now also involves the Coulomb interaction energy between vortices. However, we expect the activation energy to be essentially independent of f as in the dilute-gas regime. A crude estimate of the activation energy is given by the change in the interaction energy when displacing one vortex by a fraction of the typical separation $\ell = f^{-1/2}$. As ℓ is large compared to the lattice spacing, the Coulomb potential between the chosen vortex and the others can be taken as logarithmic, and the change in the interaction energy is then of $O(1)$ irrespective of f . [As an illustration, consider for simplicity three vortices at a distance ℓ from each other. The cost for one vortex to pass, say, through the middle of the segment joining the two other vertices to reach another equilibrium configuration is the difference between $-2\pi J \ln[\ell/(2a)]$ and $-2\pi J \ln(\ell/a)$, i.e., $4\pi J \ln(2)$.]

For even larger frustration f , ℓ becomes of the order of the lattice spacing. The system is denser and more akin to a liquid. The activation energy should then be sensitive to the density f and as in a simple liquid [25,26] increase with the density. This will be discussed below.

One can summarize the predicted behavior for the temperature dependence of the relaxation time $\tau(f, T)$ in the weakly frustrated XY model as follows:

(1) For $T_{vl}(f) \lesssim T \lesssim T^*$ with T_{vl} as a crossover temperature whose dependence on f is unknown,

$$\tau(f, T) \sim f^{-1} T^{-3/2}. \quad (10)$$

(2) For $T_{\text{crys}} < T \lesssim T_{vl}(f)$, there is a vortex liquid regime in which

$$\tau(f, T) \sim \tau_0 e^{\Delta_0/T}, \quad (11)$$

with $\Delta_0 \sim J$ is a constant activation energy that is independent of f in the limit of small frustration (and possibly increases with f for large enough frustration) and τ_0 is a T -independent but possibly f -dependent elementary time scale. The first regime is controlled by spin-wave kinetics, whereas the second one is due to the activated motion of the irreducible frustration-induced defects.

From the above predictions one can already see the difference with the glass-forming behavior of supercooled liquids, including that found in 2D curved space: No generic super-Arrhenius temperature dependence is expected for the uniformly frustrated XY model; quite the contrary,

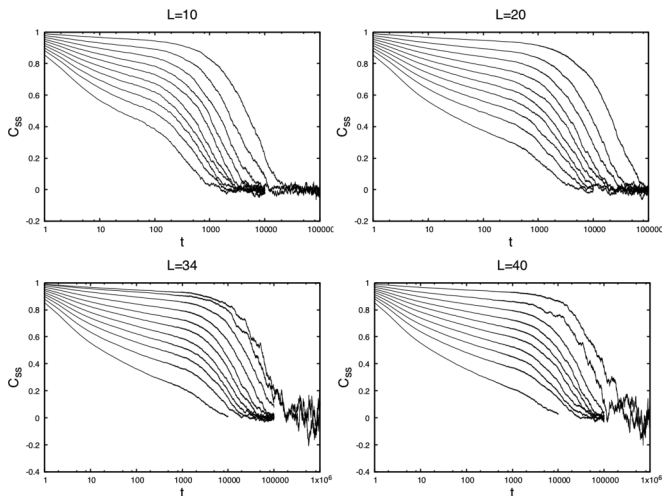


FIG. 1. Spin autocorrelation function $C_{ss}(t)$ versus $\log_{10}(t)$ for the unfrustrated ($f = 0$) 2D XY model at temperatures from $T/J = 1$ to 0.1 (from left to right: $T/J = 1.0, 0.9, 0.8, 0.7, 0.6, 0.5, 0.4, 0.3, 0.2, 0.1$) for different system sizes from $L = 10$ to $L = 40$. System size $L = 34$ includes one additional curve at $T/J = 0.13$.

a sub-Arrhenius behavior should be observed in the first temperature regime described above.

IV. SIMULATION RESULTS: THE UNFRUSTRATED CASE

The simulation results for the finite-size scaling of $C_{ss}(t)$ in the unfrustrated ($f = 0$) case are shown in Fig. 1 for several system sizes from $L = 10$ to $L = 40$. $C_{ss}(t)$ indeed exhibits an exponential decay at long times and a power-law time dependence at shorter times with an exponent that decreases as T decreases. In Fig. 2 we show a log-log plot of C_{ss} for the largest system size $L = 40$. The exponent in the power-law

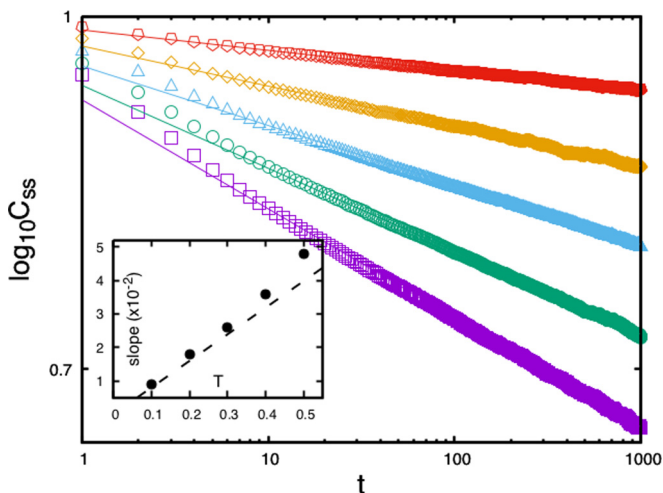


FIG. 2. Log-log plot of $C_{ss}(t)$ at short times (first regime of the data in Fig. 1) for the unfrustrated ($f = 0$) 2D XY model with $L = 40$ at several temperatures: $T/J = 0.1, 0.2, 0.3, 0.4, 0.5$ (from top to bottom). Inset: Extracted slope versus temperature. The dashed line is the predicted behavior $1/(4\pi)(T/J)$.

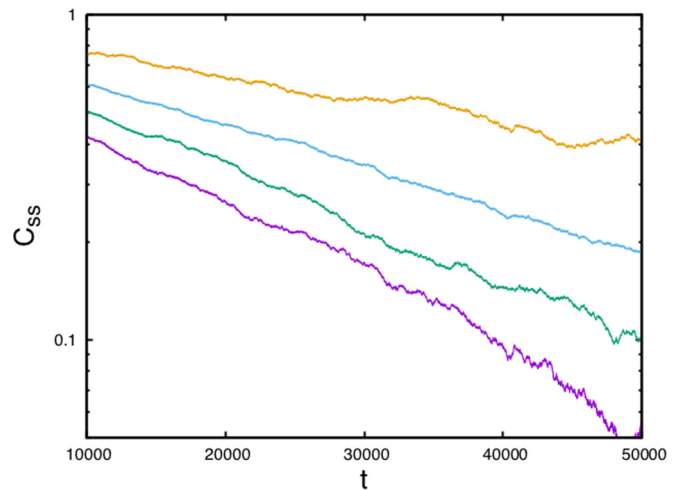


FIG. 3. Log-linear plot of $C_{ss}(t)$ at long times (second regime of the data in Fig. 1) for the unfrustrated ($f = 0$) 2D XY model with $L = 40$ at several temperatures $T/J = 0.2, 0.3, 0.4, 0.5$ from top to bottom, showing the exponential decay at long times.

regime varies linearly with temperature and is quantitatively compatible with the predicted value as shown in the inset of the figure.

From the exponential behavior in the long-time regime (see Fig. 3) we extract a relaxation time $\tau_2(L, T)$. (In practice we evaluate the slope on the log-linear plot in Fig. 3 through a least-squares fit and thereby obtain an estimate of $(\log_{10} e)/\tau_2$. In all cases the error bars from the fit are smaller than the symbol size.) This relaxation time is plotted as a function of inverse temperature for different values of the system size L in Fig. 4. As shown on the log-log plot in the inset of Fig. 4, τ_2 scales as a power-law $T^{-\gamma}$ at low enough T with the exponent

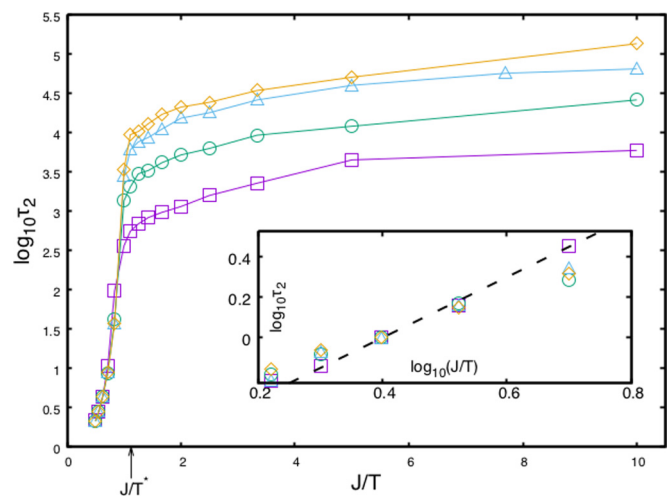


FIG. 4. Arrhenius plot of the T dependence of the relaxation time, i.e., $\log_{10} \tau_2$ versus J/T , for the unfrustrated ($f = 0$) 2D XY model for $L = 10, 20, 34, 40$ (from bottom to top). Inset: Plot of $\log_{10} \tau_2$ versus $\log_{10}(J/T)$ for $T \lesssim 0.5J$, showing a power-law behavior compatible with $T^{-3/2}$ (displayed as the dashed straight line). J/T^* denotes the BKT transition temperature.

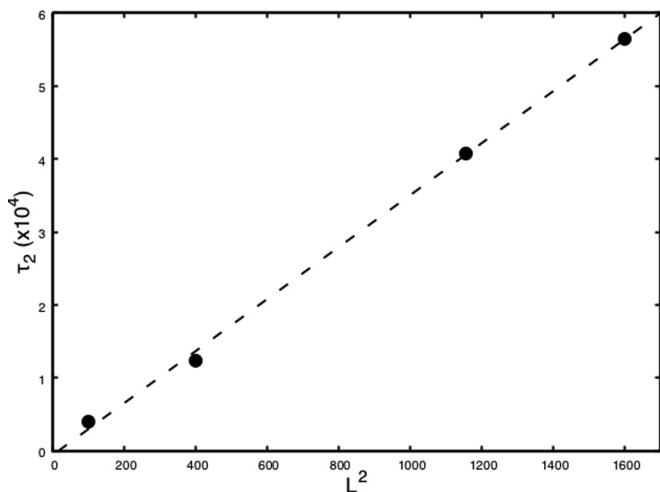


FIG. 5. Finite-size scaling in the unfrustrated ($f = 0$) 2D XY model for $L = 10, 20, 34, 40$: τ_2 versus L^2 for a low temperature of $T/J = 0.2$.

$y \approx 1.5$. Furthermore, at a fixed temperature we also find that τ_2 scales as L^2 (see Fig. 5 for $T = 0.2J$).

All these observations support the predictions presented in the previous section.

V. SIMULATION RESULTS: THE FRUSTRATED CASE

We now present the results for the (equilibrium) dynamics of the frustrated model for five different values of frustration: $f = 5/(34)^2$, $f = 10/(34)^2$, $f = 1/34$, $5/34$, and $13/34$. This corresponds to typical distances between irreducible vortices $\ell = f^{-1/2}$ of $\ell \approx 15.2$, $\ell \approx 10.8$, $\ell \approx 5.8$, $\ell \approx 2.6$, and $\ell \approx 1.6$, respectively (in units of the lattice spacing) and thus spans small to quite strong frustrations. The largest frustration $f = 13/34$ was previously numerically investigated by Kim and Lee [27] as an approximation to an irrationally frustrated model with $f =$ the golden mean, $(3 - \sqrt{5})/2$ [28]. Slow dynamics was found and claimed to be analogous to the relaxation in supercooled liquids. This will be discussed further below.

We note that the frustrated model in the range of the temperature under study has a weak dependence on system size, contrary to the unfrustrated model which is essentially always critical at and below T^* (for a similar observation, see Ref. [27]). The results shown here are for a 34×34 lattice [29].

A. Time-dependent correlation functions

The spin autocorrelation function $C_{ss}(t)$ is displayed in Fig. 6 as a function of the logarithm of time for the five frustrations and a domain of temperature from $T/J = 2 > T^*$ down to $T/J = 0.1$. As we have checked, the system stays in the disordered phase over this whole temperature regime, and the BKT transition is indeed avoided. Furthermore, as anticipated from previous studies [16,17], there is no sign of formation of an Abrikosov crystal of vortices. Equilibration takes longer as the temperature decreases, and for temperatures below $T/J = 0.1$ the system falls out of equilibrium on

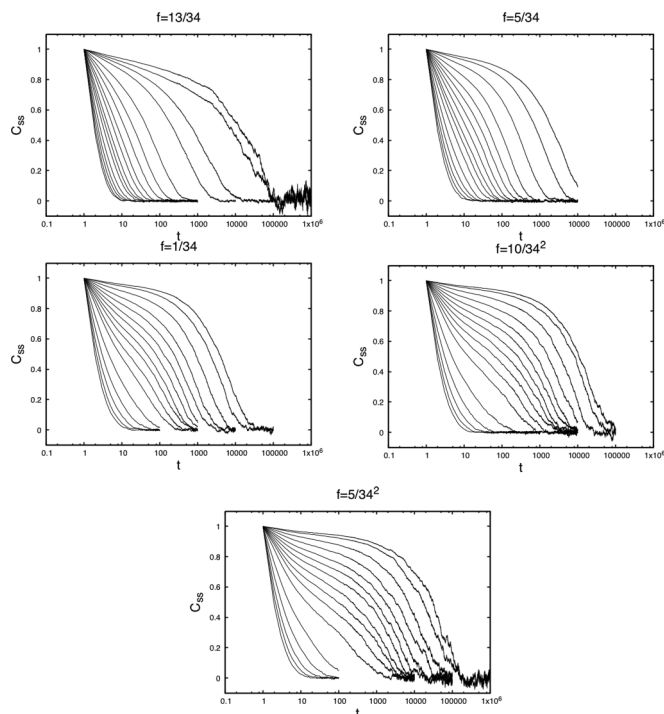


FIG. 6. Spin autocorrelation function $C_{ss}(t)$ versus $\log_{10}(t)$ for the frustrated 2D XY model at several temperatures from $T/J = 2$ down to $T/J = 0.1$ (from left to right: $T/J = 2.0, 1.8, 1.6, 1.4, 1.2, 1.0, 0.9, 0.8, 0.7, 0.6, 0.5, 0.4, 0.3, 0.2, 0.13, 0.1$) for five frustrations: $f = 13/34, 5/34, 1/34, 10/(34)^2$, and $5/(34)^2$. Frustration $f = 13/34$ includes one additional curve at a temperature of $T/J = 0.16$.

the time scale of the simulation: The system then becomes a “glass,” but we do not investigate this out-of-equilibrium glassy phase.

The shape of the function $C_{ss}(t)$ changes both as a function of temperature and as a function of frustration. For the three smallest frustrations, the behavior of $C_{ss}(t)$ appears quite similar to that of the finite-size system in the absence of frustration as can be seen by comparing Fig. 6 with Fig. 1. This is most visible in the short-time regime, before the appearance of a knee. In the long-time regime, the frustrated cases differ from the unfrustrated case; whereas the latter shows simple exponential decay at long times, the former exhibit stretched exponential behavior, $C_{ss}(t) \sim \exp[-(t/\tau)^\beta]$ with $\beta < 1$. However, the dependence of the stretching parameter β on temperature is unanticipated as β appears to increase with decreasing temperature from $\beta \lesssim 0.5$ around $T/J = 1$ to $\beta \sim 0.8$ at the lowest temperatures. This is at odds with what is found in supercooled liquids.

For the two largest frustrations $f = 5/34$ and $f = 13/34$, the behavior of $C_{ss}(t)$ changes from a simple or compressed exponential dependence at high temperatures ($T > T^*$) to a two-step relaxation with the last stage being described by a stretched exponential at low temperatures. This is similar to what was observed in Refs. [27,33]. In these two cases and contrary to what is observed for the smaller frustrations, the stretching parameter decreases as temperature decreases, in line with what is found in supercooled liquids: β goes from around 1 at $T/J = 1.2$ to 0.7 at $T/J = 0.1$ for $f = 5/34$, and

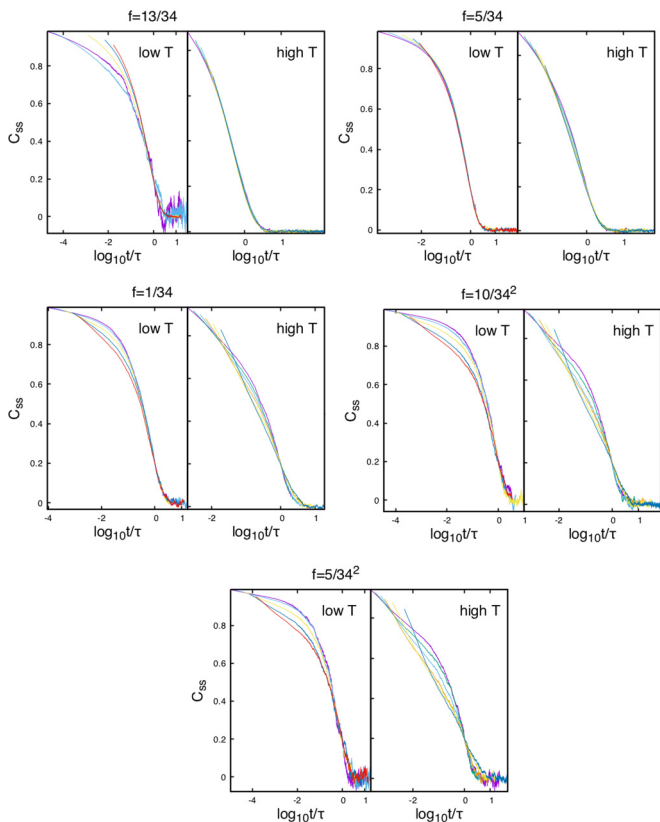


FIG. 7. Test of the so-called time-temperature superposition principle: Same data as in Fig. 6 plotted versus the logarithm of the scaled time $t/\tau(T)$. The data are divided into “high T ” and “low T ” as described in the text. Although superposition is never found for the three smallest frustrations, it is observed approximately for the two strongest at high temperatures and then violated at low temperatures.

β goes from around 1 at $T/J = 0.9$ to 0.6 at $T/J = 0.13$ for $f = 13/34$ (this is compatible with the results of Ref. [33]). Note however that the signature of the glassy regime in many simple glass formers, namely, the presence of a well-developed plateau separating two relaxation regimes, is not found in the time-dependent correlation function of the present systems.

The different types of behavior for the evolution of the shape of $C_{ss}(t)$ with temperature are also illustrated by considering plots where time t is rescaled by the relaxation time $\tau(T)$ (extracted as discussed below): See Fig. 7. The collapse on a single curve corresponds to the “time-temperature superposition.” We have divided the range of temperatures into “high T ,” $T/J = 0.5$ – 1.0 , and “low T ,” $T/J = 0.1$ – 0.4 . The cutoff between high and low T ’s was chosen such that high- T data gave the best collapse. We see that the superposition principle is never valid for the three smallest frustrations, no matter the temperature range. For the two strongest frustrations, time-temperature superposition is roughly obeyed at high T where the relaxation is essentially exponential (as discussed above, this is no longer true when going to temperatures around and above $2T^*$) but is violated at low temperatures where the relaxation is stretched and the stretching parameter decreases with decreasing T . This latter pattern is more in line with what is usually found in glass-forming liquids.

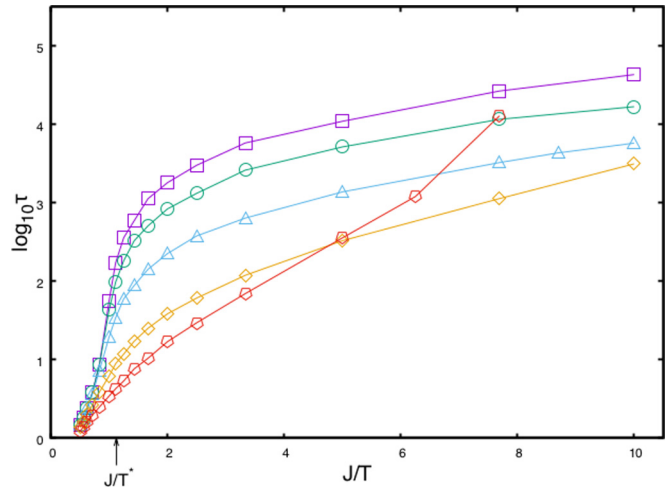


FIG. 8. Arrhenius plot of $\log_{10}(\tau)$ versus J/T for $f = 5/(34)^2, 10/(34)^2, 1/34, 5/34, 13/34$ (from top to bottom). J/T^* denotes the BKT transition temperature.

B. Temperature dependence of the relaxation time

We have determined the relaxation time τ either as the time at which the autocorrelation function is equal to 0.2 or as the parameter entering in the stretched-exponential description of the long-time decay. Very similar values are found through the two procedures, and below we illustrate the trend with temperature by using the second prescription (stretched-exponential fit).

The logarithm of the relaxation time τ is shown in Fig. 8 as a function of J/T for the five frustrations. The relaxation time increases with decreasing temperature, but the dependence is quite different from what is seen for glass-forming liquids: In place of a super-Arrhenius dependence with a positive curvature on the Arrhenius plot, one first finds an opposite trend with a rapid increase followed by some form of sub-Arrhenius behavior at intermediate temperatures and finally, when accessible, a low- T Arrhenius regime.

This behavior qualitatively corresponds to what we have predicted in Sec. III. The increase followed by a sub-Arrhenius dependence corresponds to the power-law temperature dependence predicted by Eq. (10). To check this in more detail we display a log-log plot of $\tau(T)$ in Fig. 9. As shown in the figure, the intermediate-temperature regime can indeed be fitted by a power-law behavior, but we find that the effective exponent extracted from the slope varies with frustration: It increases from about 1.9 for the smallest frustration $f = 5/(34)^2$, a value that is not too far from the exponent $3/2$ predicted in Eq. (10), to 2.2–2.3 for the largest ones. (The results are very similar when extracting τ from the other prescription: The values of the effective exponent are within 5% of the stretched-exponential results.)

We can rationalize the observed behavior as follows. For the smallest frustrations the activation energy is likely small enough that it is hard to disentangle Arrhenius from power-law dependence over the temperature range under study: Recall that the estimate of the activation energy [see Eq. (11)] when $f \rightarrow 0^+$ is $0.19J$ so that the activated Arrhenius factor in $\tau(T)$ stays of $O(1)$ for $T \gtrsim 0.1$. Actually, a fit to the last three

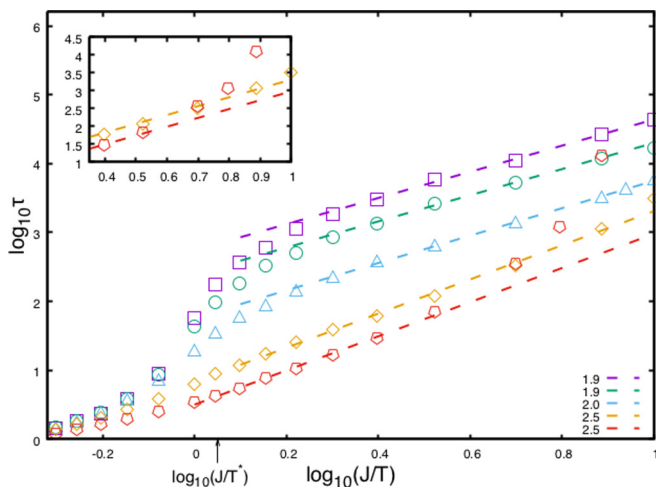


FIG. 9. Log-log plot of τ versus J/T . Same data as in Fig. 8: $f = 5/(34)^2, 10/(34)^2, 1/34, 5/34, 13/34$ (from top to bottom). The dashed lines are linear fits to the data with slopes given in the figure. Inset: Zoom on the low- T region for the two largest frustrations $f = 5/34$ and $f = 13/34$. J/T^* denotes the BKT transition temperature.

points of the Arrhenius plot in Fig. 8, for $5 \leq J/T \leq 10$, gives an effective activation energy on the order of 0.24 – $0.28J$ for the frustrations $f \leq 1/34$. For these frustrations it then seems reasonable to assign the increase in the effective exponent of the power-law fit to the presence of a very smooth crossover to the Arrhenius regime.

Over the temperature range that we can access, i.e., $T \geq 0.1J$, a crossover to an Arrhenius behavior is unambiguously detected only for the two largest frustrations $f = 5/34$ and $f = 13/34$. This can be seen from the deviation from the power-law fit at low T in the inset of Fig. 9, with a crossover temperature T_{vl} around $0.2J$ [$\log_{10}(J/T) \approx 0.7$] for $f = 5/34$ and around $0.3J$ [$\log_{10}(J/T) \approx 0.5$] for $f = 13/34$. The range over which the power-law fit is good appears to extend to lower temperatures as f decreases, so that the Arrhenius regime is too weak or out of reach for $f \leq 1/34$.

Interestingly, the crossover T_{vl} does not seem to correlate with the temperature at which virtually all thermal defects have disappeared, and only the irreducible vortices induced by the flux f remain. One can see from Fig. 10 that this temperature is found rather around $T \approx 0.7J$, irrespective of the value of f . This temperature is better correlated with the establishment of the power-law regime [see Fig. 9 with $\log_{10}(0.7) \approx 0.155$].

For the two largest frustrations we find, as argued in Sec. III, that the activation energy increases with f : It is equal to $0.45J$ for $f = 5/34$ and to $1.2J$ for $f = 13/34$ (and is larger than the estimate for small frustrations with $E \sim 0.2$ – $0.3J$). This effect is similar to the increase of the activation energy found in a liquid with increasing density. Similar values of the order of J have also been obtained in rather strongly frustrated XY models in the temperature regime below $T/J \approx 0.2$. The data of Kim and Lee [27] for $f = 13/34$ can be fitted below $T \approx 0.25$ – $0.2J$ with a low-temperature activation energy of $E \approx 1.3J$. (The authors try to describe the T dependence by a super-Arrhenius dependence, but, as shown in Fig. 8, the

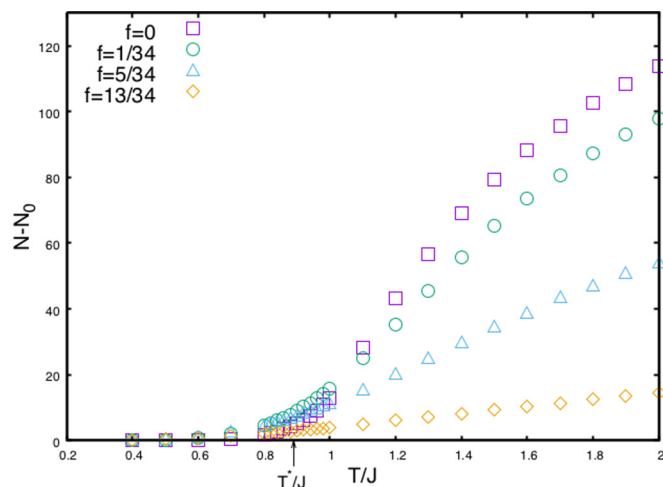


FIG. 10. Number of vortices N minus the number of irreducible vortices N_0 for $f = 1/34, 5/34, 13/34$ and for $f = 0$ with $L = 40$ (the number of irreducible vertices is 34, 170, 442, and 0, respectively). At $T \approx 0.7J$ and below the thermal vortices have virtually disappeared. T^*/J denotes the BKT transition temperature.

super-Arrhenius character is not significant and tends to be mixed with the crossover with the power-law regime.) In the fully frustrated XY model ($f = 1/2$), Granato [34] observes Arrhenius behavior with $E \approx 1.0J$, and in a related model of a curvature-induced frustrated XY model on a hyperbolic lattice with $f = -1/6$ (see also below), Baek *et al.* [35] found $E \approx 0.92J$.

Note finally that the curves appear to converge at high temperatures above T^* : See Figs. 8 and 9. This is expected from the picture of a frustrated model being like an unfrustrated one in a finite-size $L \sim \ell$. (For the two largest frustrations there are small deviations for temperatures higher than those shown in Figs. 8 and 9, but this merely reflects the fact that the characteristic length ℓ , which is then equal to 1.6 for $f = 13/34$ and 2.6 for $f = 5/34$, is so small that bulk behavior is not recovered.)

C. Spin-wave kinetics versus activated vortex motion

We have computed the current autocorrelation function $C_{jj}(t)$ to see whether the dynamics of the currents couples differently than that of the spins to the two relaxation mechanisms associated with spin waves and with the frustration-induced irreducible defects, respectively. One indeed expects that, in the case of a complete decoupling between the spin waves and the defects (as in the Villain model [36]), $C_{jj}(t)$ would mostly probe the activated motion of the irreducible vortices rather than the spin-wave kinetics and could be significantly slower than that of the spin autocorrelation function $C_{ss}(t)$. However, over the range of time and temperature that we could access, this is not what we have observed. As illustrated by the log-linear plot in Fig. 11 for $f = 1/34$ at $T/J = 0.3$, $C_{jj}(t)$ rather has a more rapid decay than $C_{ss}(t)$: This is apparent at short times (say for $t < 100$ in Fig. 11), whereas at longer times the two functions appear to decay more in parallel with, however, a slightly faster rate for $C_{jj}(t)$

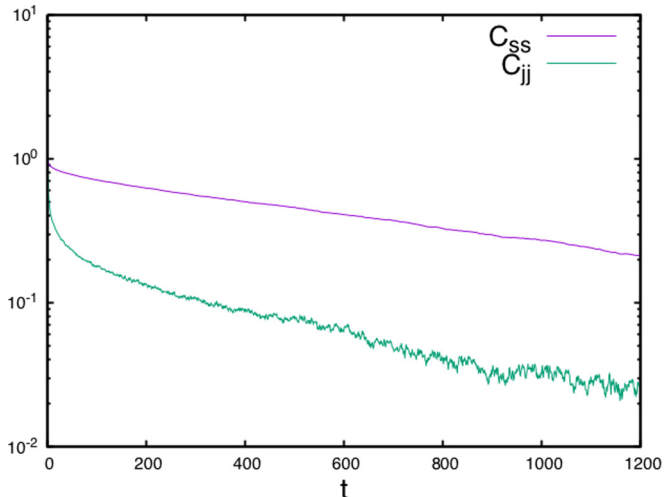


FIG. 11. Comparison of the time-dependent spin and current autocorrelation functions for $f = 1/34$ and $T/J = 0.3$. The latter has a faster initial decay, but the relaxation times describing the final relaxation stage are comparable.

(see also Fig. 12). The absence of any additional slower relaxation in the current autocorrelation function is in line with what was found in Ref. [27] where the time-dependent vorticity autocorrelation function (directly sensitive to the vortices) and the spin autocorrelation function show a similar behavior.

To gain more insight, we have considered a system in which the frustration-induced vortices are pinned. We do so for $f = 1/34$ at several temperatures, $T/J = 0.7, 0.5, 0.3$, for which virtually all thermally induced vortices have disappeared (see Fig. 10). We have then computed both the current and the spin time-dependent autocorrelation functions.

In the top panel of Fig. 12 we compare $C_{jj}(t)$ in the presence and in the absence of a vortex pinning potential. The first rapid decay is similar in the two cases but, quite notably, the current autocorrelation function does not decay to zero in the presence of pinned vortices, whereas it does in the unpinned case. (The height of the plateau at long times increases roughly linearly as temperature decreases as one would expect as a result of the linear increase of the spin stiffness.) This clearly indicates that the long-time decay of $C_{jj}(t)$ in the unpinned case is due to the motion of the frustration-induced vortices. At the same time as shown in the bottom panel of Fig. 12, the spin autocorrelation function $C_{ss}(t)$ decays to zero whether vortices are pinned or not. The initial part of the decay is similar in the two cases, but the final, and main, relaxation is significantly slower when the frustration-induced defects are pinned. Pinning the vortices therefore slows down the dynamics but does not prevent full relaxation of the spins.

These observations seem to confirm that, in this temperature range, which according to Fig. 9 corresponds to a power-law temperature dependence of the relaxation time, the dynamics of the currents is controlled by the motion of the frustration-induced vortices, whereas that of the spins is dominated by spin-wave kinetics. This makes the above finding about the comparable decay rate at long times of $C_{jj}(t)$ and $C_{ss}(t)$ in the

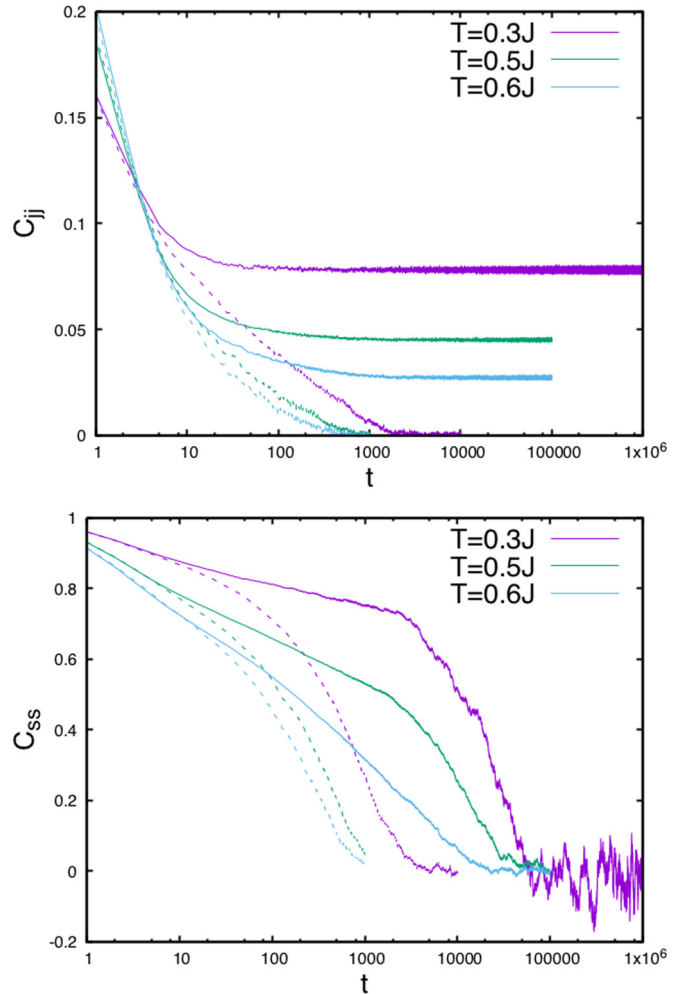


FIG. 12. Effect of pinning the frustration-induced vortices in the uniformly frustrated XY model for $f = 1/34$ at several temperatures, $T/J = 0.6, 0.5, 0.3$: Time-dependent current (top) and spin (bottom) autocorrelation functions in the system with and without vortex pinning. The solid lines are with vortex pinning, and the dashed lines are without vortex pinning.

absence of vortex pinning even more surprising. This appears to imply that the two mechanisms at play, spin-wave kinetics and irreducible-vortex motion, have similar time scales in the temperature regime under consideration.

VI. DISCUSSION

We have found that the frustration-induced avoidance of the BKT transition in a uniformly frustrated 2D XY model generates slow relaxation and complex dynamics in the system at temperatures near and below the avoided transition. However, the characteristics of this relaxation slowdown are qualitatively different than that found in glass-forming liquids. In particular, the super-Arrhenius temperature dependence of the relaxation time that is commonly observed in supercooled liquids is not reproduced by the present model (see the Introduction). Taken at face value, this means that small frustration and avoided criticality are not sufficient to generate

the phenomenology associated with the glass transition. More ingredients are necessary.

Of special interest then is to contrast the properties of the 2D uniformly frustrated XY model with those of atomic liquids in 2D curved space. The scenario of “frustration-avoided criticality” [7,8] is also realized by a one-component simple atomic liquid in two-dimensional curved space. With decreasing temperature, the liquid in Euclidean space easily goes into an ordered or quasicrystalline phase with sixfold symmetry: Depending on the nature of the interaction potential, the liquid crystallizes in a hexagonal phase through one weakly first-order transition or through a sequence of two continuous or weakly first-order transitions separated by a narrow bond-orientationally ordered hexatic phase [6,37]. However, curving space, i.e., embedding the liquid in a 2D manifold of constant curvature, thwarts crystallization. The prevalent local order has a sixfold symmetry (hexatic or hexagonal order), but its spatial extension is frustrated by the nonzero curvature [6,11], which then plays the role of the flux f in the frustrated XY model. The transition or sequence of ordering transitions at or around a temperature T^* is avoided because curvature imposes an irreducible density of topological defects, “disclinations” and “dislocations” in the underlying hexatic/hexagonal medium: The system stays in the liquid phase even below T^* and only (possibly) encounters a defect-ordering phase transition at a much lower temperature where the irreducible defects form a lattice. One-component atomic liquids can therefore be supercooled by applying curvature and can subsequently form a glass.

These model glass-forming liquids in curved space have been investigated by analytical and numerical means both for constant negative curvature (the hyperbolic plane H^2 that is of infinite extent and cannot be embedded in 3D Euclidean space) [11,12] and for constant positive curvature (the more familiar sphere S^2 of finite extent) [38]. It was found that crystallization is indeed avoided and that the dynamics of the “supercooled” liquid slows down as one lowers the temperature below T^* at constant curvature. However, contrary to what we observe here for the uniformly frustrated XY model, the relaxation time apparently displays a super-Arrhenius temperature dependence. The “fragility,” which characterizes how quickly the relaxation time and the transport coefficients increase with decreasing temperature [39], changes with the curvature, i.e., the frustration: The more frustrated, the less fragile. Other characteristics of the relaxation slowdown in glass-forming liquids, such as the marked nonexponential time dependence of the relaxation functions and the increasingly heterogeneous character of the dynamics with the coexistence over an extended period of time of fast and slow regions [2,3], are also observed.

Why are the dynamics of liquids in curved space and uniformly frustrated XY systems so different despite the fact that the spatial dimension of the manifold is the same? The frustration f is of course not produced by the same mechanism in the two cases, being associated with the curvature in the former and with the flux in the latter. However, Baek *et al.* [35] have studied, with Monte Carlo simulations, the XY model on a hyperbolic lattice in which a uniform frustration with $f = -1/6$ (corresponding to a typical frustration length of $\ell \approx 2.45$) is generated by the curvature. The model

shows no significant differences with the uniformly frustrated XY model in flat space with a similar frustration length (i.e., our study for the largest frustrations). In particular, it does not display the super-Arrhenius behavior found for the liquid.

The difference seems to rather stem from the nature of the degrees of freedom: spins in one case, with phase fluctuations (i.e., spin waves) and vortex fluctuations; particles in the other, with both translational and bond-orientational fluctuations and the associated defects, dislocations, and disclinations. Disclinations are akin to vortices in the XY model. Dislocations, however, have been argued to play a crucial role in the physics of liquids in curved space at low enough temperatures, including the relaxation via thermal activation [12]. They have no direct counterparts in the uniformly frustrated XY model at low temperatures. It is then possible that the latter system misses this important piece of liquid physics, the intertwining of translational and rotational degrees of freedom, and displays a relaxation slowdown associated with avoided criticality that is too dominated by spin-wave kinetics to be a minimal model for generic glass-forming liquids.

Further evidence pointing to a qualitative difference between the 2D uniformly frustrated XY model and 2D glass-forming liquids comes from the role of “soft modes” in the dynamics. The latter are the remains of the long-wavelength excitations present in the absence of frustration, i.e., spin waves in the XY model and density fluctuations in liquids, which have a drastic influence on the ordering behavior in two-dimensional systems [40]. These soft modes have recently been shown to have a strong effect on the dynamics of 2D glass-forming liquids [41–45]. However, they can be disentangled from the more proper glassy component of the dynamics, which then appears similar to what is generically found in 3D supercooled liquids [42–45]. This is in contrast to what we have found here in the case of the uniformly frustrated XY model.

Based on the above discussion, one may then wonder whether there are generalizations of the 2D uniformly frustrated models that are better suited for describing glass-forming liquids and yet still tractable, and, more generally, what are the additional ingredients to be added to frustration-avoided criticality to produce a minimal theory of glass formation. Whether or not this is possible is yet to be seen. It could be that a theory based on small frustration and avoided criticality is not the best zeroth-order description of glass formation. This discussion however goes beyond the scope of this paper.

Finally, it is worth mentioning that the uniformly frustrated 2D XY model studied in this paper has experimental realizations either in the form of arrays of Josephson junctions or of periodic networks of superconducting wires and that the relaxation of the system can therefore be accessed experimentally as a function of both temperature and frustration. There have been many studies of this kind in the past [46–52], focusing, for instance, on the resistive behavior of the system, but most of them focused on either the very low-temperature regime where a transition to an ordered vortex phase may appear or to the immediate vicinity of the BKT transition. A consistent experimental description of the whole temperature range as a function of frustration, i.e., magnetic flux, would therefore be of great interest.

ACKNOWLEDGMENTS

We would like to thank S. Raghu for collaboration during the early stages of this work. I.E. and S.A.K. were supported by the U.S. Department of Energy,

Office of Basic Energy Sciences under Contract No. DE-AC02-76SF00515. Computational work was performed on the SLAC and Sherlock clusters at Stanford University.

-
- [1] S. A. Kivelson and G. Tarjus, *Nat. Mater.* **7**, 831 (2008).
- [2] L. Berthier and G. Biroli, *Rev. Mod. Phys.* **83**, 587 (2011).
- [3] G. Tarjus, in *Dynamical Heterogeneities and Glasses*, edited by L. Berthier, G. Biroli, J.-P. Bouchaud, L. Cipelletti, and W. van Saarloos (Oxford University Press, New York, 2011).
- [4] F. C. Frank, *Proc. R. Soc. London, Ser. A* **215**, 43 (1952).
- [5] J.-F. Sadoc and R. Mosseri, *Geometrical Frustration* (Cambridge University Press, Cambridge, UK, 2006).
- [6] D. R. Nelson, *Defects and Geometry in Condensed Matter Physics* (Cambridge University Press, Cambridge, UK, 2002).
- [7] G. Tarjus, S. A. Kivelson, Z. Nussinov, and P. Viot, *J. Phys.: Condens. Matter* **17**, R1143 (2005).
- [8] D. Kivelson, S. A. Kivelson, X. Zhao, Z. Nussinov, and G. Tarjus, *Physica A* **219**, 27 (1995).
- [9] L. Chayes, V. J. Emery, S. A. Kivelson, Z. Nussinov, and G. Tarjus, *Physica A* **225**, 129 (1996).
- [10] Note that contrary to what is observed in two dimensions, crystallization is usually strongly first order in three-dimensional Euclidean space. However ordinary crystallization is not the avoided ordering transition we have in mind. Indeed, the discontinuous character may be, in part, a consequence of strong frustration. The theory is based upon the assumed existence of an “ideal ordering transition.” The icosahedral ordering in the $\{3,3,5\}$ polytope on the surface S^3 of a four-dimensional hypersphere looks like a finite-size first-order transition, but on the other hand the ordering transition of parallel cubes in Euclidean three-dimensional space is a second-order transition (in the universality class of the 3D XY model) [53–55]. We expect that the absence of frustration will favor a continuous or weakly first-order transition [7].
- [11] F. Sausset, G. Tarjus, and P. Viot, *Phys. Rev. Lett.* **101**, 155701 (2008); F. Sausset and G. Tarjus, *ibid.* **104**, 065701 (2010).
- [12] F. Sausset, G. Tarjus, and D. R. Nelson, *Phys. Rev. E* **81**, 031504 (2010).
- [13] S. Teitel and C. Jayaprakash, *Phys. Rev. Lett.* **51**, 1999 (1983).
- [14] S. Teitel, in *40 Years of Berezinskii-Kosterlitz-Thouless Theory*, edited by J. V. José (World Scientific, Singapore, 2013), Chap. 6, p. 201.
- [15] D. S. Fisher, *Phys. Rev. B* **22**, 1190 (1980).
- [16] M. Franz and S. Teitel, *Phys. Rev. B* **51**, 6551 (1995).
- [17] S. A. Hattel and J. M. Wheatley, *Phys. Rev. B* **51**, 11951 (1995).
- [18] This is more subtle when considering a finite system with periodic boundary conditions as we do here. There may then be an additional dependence on large-scale vorticity associated with loops wrapping around the system [20]. For the local quantities that we consider in this paper this dependence is, however, absent. In addition the periodic boundary conditions may frustrate the establishment of an ordered (or quasiordered) phase of irreducible vortices, but this is not relevant in the temperature domain under study where the system remains significantly above any transition to such ordered phases.
- [19] P. C. Hohenberg and B. I. Halperin, *Rev. Mod. Phys.* **49**, 435 (1977).
- [20] V. Alba, A. Pelissetto, and E. Vicari, *J. Phys. A: Math. Theor.* **41**, 175001 (2008).
- [21] This is obtained simply by taking into account spin-wave contributions down to a wave-vector $q = (2\pi/L)$ while dropping the $q = 0$ mode: See, e.g., Ref. [22].
- [22] S. T. Bramwell and P. C. W. Holdsworth, *J. Phys.: Condens. Matter* **5**, L53 (1993).
- [23] J. Daligault, *Phys. Rev. Lett.* **96**, 065003 (2006).
- [24] C. J. Lobb, D. W. Abraham, and M. Tinkham, *Phys. Rev. B* **27**, 150 (1983).
- [25] S. Sastry, *PhysChemComm* **3**, 79 (2000).
- [26] G. Tarjus, D. Kivelson, S. Mossa, and C. Alba-Simionesco, *J. Chem. Phys.* **120**, 6135 (2004).
- [27] B. Kim and S. J. Lee, *Phys. Rev. Lett.* **78**, 3709 (1997).
- [28] T. C. Halsey, *Phys. Rev. Lett.* **55**, 1018 (1985).
- [29] Note that we are not interested in establishing and studying the presence of a low-temperature (ordered, quasiordered, or glassy) phase as we work at temperatures significantly above the putative transition: See Refs. [16,17] for the small-frustration cases. For the stronger frustration $f = 13/34$, which is an approximant to the irrational frustration given by the golden mean, the situation is more controversial [27,28,30–32]. It has, for instance, been argued that there is a zero-temperature transition with associated finite-size effects [32]. However, for the temperature range and the system sizes that we study these effects are negligible.
- [30] E. Granato, *Phys. Rev. B* **54**, R9655 (1996).
- [31] P. Gupta, S. Teitel, and M. J. P. Gingras, *Phys. Rev. Lett.* **80**, 105 (1998).
- [32] S. Y. Park, M. Y. Choi, B. J. Kim, G. S. Jeon, and J. S. Chung, *Phys. Rev. Lett.* **85**, 3484 (2000).
- [33] M. R. Kolarhchi and H. Fazli, *Phys. Rev. B* **62**, 9089 (2000).
- [34] E. Granato, *Phys. Rev. B* **85**, 054508 (2012).
- [35] S. K. Baek, H. Shima, and B. J. Kim, *Phys. Rev. E* **79**, 060106(R) (2009).
- [36] J. Villain, *J. Phys. France* **36**, 581 (1975).
- [37] E. P. Bernard and W. Krauth, *Phys. Rev. Lett.* **107**, 155704 (2011); S. C. Kapfer and W. Krauth, *ibid.* **114**, 035702 (2015).
- [38] J.-P. Vest, G. Tarjus, and P. Viot, *Mol. Phys.* **112**, 1330 (2014).
- [39] C. A. Angell, *J. Non-Cryst. Solids* **131-133**, 13 (1991).
- [40] N. D. Mermin and H. Wagner, *Phys. Rev. Lett.* **17**, 1133 (1966); N. D. Mermin, *Phys. Rev.* **176**, 250 (1968).
- [41] E. Flenner and G. Szamel, *Nat. Commun.* **6**, 7392 (2015).
- [42] H. Shiba, Y. Yamada, T. Kawasaki, and K. Kim, *Phys. Rev. Lett.* **117**, 245701 (2016).
- [43] S. Vivek, C. P. Kelleher, P. M. Chaikin, and E. R. Weeks, *Proc. Natl. Acad. Sci. USA* **114**, 1850 (2017).
- [44] B. Illing, S. Fritschi, H. Kaiser, C. L. Klix, G. Maret, and P. Keim, *Proc. Natl. Acad. Sci. USA* **114**, 1856 (2017).
- [45] G. Tarjus, *Proc. Natl. Acad. Sci. USA* **114**, 2440 (2017).

- [46] J. P. Carini, *Phys. Rev. B* **38**, 63 (1988).
- [47] T. S. Tighe, A. T. Johnson, and M. Tinkham, *Phys. Rev. B* **44**, 10286 (1991).
- [48] F. Yu, N. E. Israeloff, A. M. Goldman, and R. Bojko, *Phys. Rev. Lett.* **68**, 2535 (1992).
- [49] S. G. Lachenmann, T. Doderer, D. Hoffmann, R. P. Huebener, P. A. A. Booi, and S. P. Benz, *Phys. Rev. B* **50**, 3158 (1994).
- [50] H. S. J. van der Zant, M. N. Webster, J. Romijn, and J. E. Mooij, *Phys. Rev. B* **50**, 340 (1994).
- [51] K. Harada, O. Kamimura, H. Kasai, T. Matsuda, A. Tonomura, and V. V. Moshchalkov, *Science* **274**, 1167 (1996).
- [52] I.-C. Baek, Y.-J. Yun, and M.-Y. Choi, *Phys. Rev. B* **69**, 172501 (2004).
- [53] J. P. Straley, *Phys. Rev. B* **30**, 6592 (1984).
- [54] F. Turci, G. Tarjus, and C. P. Royall, *Phys. Rev. Lett.* **118**, 215501 (2017).
- [55] E. A. Jagla, *Phys. Rev. E* **58**, 4701 (1998).